Residual Stresses/Strains Analysis of MEMS

Tai-Ran Hsu and Nansheng Sun

Department of Mechanical and Aerospace Engineering
San Jose State University
San Jose, CA 95192-0087

ABSTRACT

This paper describes the development of a finite element based MEMPACK code developed by the lead author and his graduate students. The MEMPACK code will be used for simulation and prediction of residual stresses and strains induced in microelectromechanical (MEM) devices during fabrication. It will also be used for the packaging design of MEMS. A case study is presented to illustrate the significant residual stresses and strains induced in a MEM device by a fabrication process.

Keywords: stress, strain, MEMS, FEM

Introduction

The success of microelectronic fabrication technologies and the wide applications of microelectronics have prompted the rapid development of MEM technology in the last decade. New applications of MEM products have continuously emerged with growing markets in consumer products, automobile, defense, space telecommunication, machine tool and manufacturing industries. The revenue generated by MEM systems (MEMS) will reach $14 billion by the end of this century, but the revenue for the industrial products enhanced by MEMS will reach $100 billion [1].

A common definition of micromachining is a way to produce MEMS materials processing of features between 1 μm and 1 mm [2]. Precision in finished dimensions and dimensional stability are extremely important for MEMS components. Minute distortions by the inherent residual strains induced by the fabrication processes could either cause misfit, or malfunctioning of the device. Additionally, most microstructures used in MEMS are made of brittle materials, e.g. silicon, and with undesirable aspect ratios in geometry. They are vulnerable to premature structural fracture. The importance of residual stresses in MEM structure design is a well-recognized factor [3]. Residual stresses induced by manufacturing processes can cause malfunctions of devices that rely on accurate stress input signals for their performance, such as micro pressure sensors.

Numerous MEMS and products of micro-valves, sensors and actuators have been developed in the last five years. Detailed descriptions of the features and functions of these micro devices can be found in trade magazines and archive journals such as ASME and IEEE transactions.

However, a search of literature in IEEE/ASME Journal of Microelectromechanical Systems for the last six years has shown no report on the mechanics of MEMS and mechanical design of MEM devices. An early attempt was made to use the finite element method for stress analysis of micro sensors as reported in reference [4]. An effort was also made by a group of experts to develop computer-aided design of MEMS [5]. the same article also dealt various issues related to the design of this type of structure. Description of a commercially available computer code called MEMCAD 3.1 can be found in a recent issue of Mechanical Engineering [6].

Current research effort by the lead author and his graduate students involves the development of a methodology that will account for the residual stresses and/or strains induced in the MEM components during fabrication processes. Such residual stresses and strains must be accounted as the input to the subsequent mechanical design analysis of MEMS components. The outcome of this research will thus contribute to the bulk knowledge that is required in design verifications of MEMS and devices.

The Need for Residual Stresses/Strains Analysis

The focus of the present research has been placed on the development of two essential algorithms that can be used to simulate the mechanistic behavior of materials subjected to micro fabrication processes. These algorithms will be incorporated into an existing TEPSAC finite element code for predicting the residual stresses and strains induced in MEMS during these fabrication processes. Residual stresses, electrostatic forces and frictions have been identified as three critical research areas in MEMS mechanics. The latter two are critical in the design of micro motors, actuators and valves. Residual stress build up in materials during fabrication is a well-known fact [3]. Excessive residual stress in the finished micro device components not only could cause premature structural failure, but also would seriously affect the functioning of the device. The associated residual strains will result in misfit of components in the delicate assembly of the device. They may also affect the performance of the device due to the

distortion and unexpected deformation of the components.

Causes for Residual Stresses/Strains

From a mechanistic point of view, residual stresses and strains are induced in a structure after excessive plastic deformation. Many currently available micro fabrication processes involve the application of intense heat (e.g. laser drilling [7], oxidation and fusion bonding [8]), or chemical effects (e.g. etching) applied to delicate materials, such as silicon substrates. Unfortunately, such intense effects almost always happen locally either near the edges or at the surfaces of the material. With these localized thermal-chemical effects, residual stresses and stains are likely to be introduced in the micro components after the fabrication processes. This phenomenon was demonstrated in one of the lead author's previous publications on laser treatment of materials [9]. Another principle source of introducing residual stresses and strains in microstructure components is due to mismatch of thermal expansion coefficients of bonded materials. For example, the formation of SiO_2 layer over silicon substrates at elevated temperature will result in tensile residual stress in the silicon substrate after the new bi-layer material is cooled down to room temperature. A significant bulge can be expected in the material as a result of the inherent residual strain. The introduction of residual stresses due to anisotropy of crystal orientations, which can occur in some micro fabrication processes, is another well-known phenomenon. Residual stresses can also be introduced in substrate materials such as silicon by ion implantation: e.g. boron as indicated in reference [10].

Current MEMS Manufacturing Processes

Common manufacturing processes used in producing MEM products include (1) bulk micromanufacturing, (2) surface micromachining and (3) LIGA and SLIGA processes [3,10,11]. The fundamental principle of bulk manufacturing involves partial removal of substrate or other materials. It is thus referred to as a "subtractive process". Almost all these processes involve one or several of the following material treatments:

(a) Electrochemical or plasma etching.
(b) Ion implantation (doping, p-n junctions).
(c) Fusion bonding.
(d) Thermochemical diffusion, e.g. oxidation.
(e) Deposition using thin or thick films and electrochemical deposition or electroplating
(f) Machining and drilling using laser, ion beam, X-ray and UV sources.

Simulation of these fabrication processes requires sophisticated nonlinear thermomechanical analysis. The finite element method is regarded as a viable approach for such purposes.

Finite Element Formulation on Nonlinear Thermomechanical Analysis

Formulation for nonlinear finite element analysis for the TEPSAC (ThermoElastic-Plastic Stress Analysis with Creep) code is presented in detail in reference [12]. The code has the following features:

(1) It handles 2-dimensional planar and 3-dimensional axisymmetrical simplex elements.
(2) The analysis is based on incremental plasticity theorem. Polynomial approximations for stress vs. strain curves of materials are used in the analysis.
(3) von Mises yield criterion is used to formulate the plastic potential function. The yield surface expands or contracts with temperature variations.
(4) Both isotropic hardening and kinematic hardening rules are included in the analysis. The latter hardening rule is useful for cyclic thermomechanical loading situations.
(5) Temperature-dependent material properties are allowed.
(6) Special features include (a) the "breakable elements" for crack growth [13] and (b) coupled thermomechanical algorithm for mechanical deformation induced thermal fields [14].Fonts and Spacing

Finite Element Analysis Simulation of Micro Fabrication Processes:

The existing "breakable elements" in the TEPSAC code [12,13] will be modified for this purpose. These elements are regarded as "pseudo elements" which are to be removed in the case of "subtractive processes", or be added for the "Additive processes".

(A) Simulation of surface micromachining:

Surface micromachining is an "additive" process. The FE mesh will include two parts:

(a) The part with real elements for substrate materials, and (b) the part with pseudo elements for added materials by various forms of "deposit", "electroplating" or "fusion bonding" in surface micro machining.

The "pseudo elements" that will be used in the code are called "A-elements" (stands for "additive elements"). Following procedure will simulate the surface micromachining using "A-elements"

(a) The "A-elements" are included in the initial FE mesh. Thickness of the region with "A-elements" = the thickness of layers of additive materials to be built on the substrate.
(b) Initial material properties assigned to the "A-elements" are:
Low Young's modulus, E; High yield stress, σ_y
Linear thermal expansion coefficient, $\alpha_{substrate}$;
Low mass density, ρ
(c) Real material properties are assigned to the "A-elements" after one pass of "deposition" or "electroplating" or "fusion bonding" is completed.
(d) Compute stress distribution in the overall FE mesh with one "A-element" of **real** layer material properties, while the rest "A-elements" still have pseudo properties. In such case, the element stiffness matrix is calculated according to:

$$[k] = \int_v [B]^T [C_{ep}][B] dv \qquad (1)$$

where [B] = matrix relates element strains and corresponding nodal displacements; $[C_{ep}]$ = elastoplasticity matrix.

Formulations of both $[B]$ and $[C_{ep}]$ matrices are available in reference [12].

(e) Update stresses, strains and nodal coordinates.
(f) Update [B] and then the stiffness matrix, $[k]$.
(g) Repeat the computation for the next surface "layer" addition.

(B) Simulation of bulk fabrication:

Bulk fabrication is a "subtractive" process. The "pseudo elements" used in this simulation will be referred to as the "S-elements" (stands for "subtractive elements").

(a) "S-elements" are included in the FE mesh for the parts that are to be etched.
(b) Initial properties assigned to the "S-elements" are identical to those of the substrate.
(c) Etch front in "S-elements" are identified according to etching rates used in the process.
(d) The $[B]$ matrix that relates element strains and the corresponding nodal displacements is adjusted according to the position of etching front with temporary assigned nodal coordinates. The reduced element stiffness is computed according to:

$$[\Delta k] = \int_{v'} [B']^T [C_{ep}][B'] dv \qquad (2)$$

in which [B'] is computed with temporary nodal coordinates.

(e) The entire "S-element" is switched to pseudo element with pseudo material properties once the etching front passed one end to the other in the element.
(f) Pseudo material properties are:
Low $[k]$ ($=10^{-6}$), Low E, High σ_y, $\alpha_{substrate}$, Low ρ.
(g) Repeat the same procedure until a converged solution is reached.
(h) Repeat the same procedure for the subsequent etching.

Case Study

A case study is presented to illustrate the residual stresses and strains introduced in a MEM device by a simple fabrication process. The case is related to the fabrication of a thin silicon membrane used for a pressure sensor. The geometry and dimensions used in the study were purposely set differently from published sensor design, so readers should not compare the present case with any pressure sensors that are in the market place.

By referring to Fig. 1, the process began with a square silicon substrate block of 2500 μm x 2500 μm x 500 μm thick (Fig. 1(a)). A 4 μm thick silicon oxide (SiO_2) layer was developed on to one surface of the substrate by a process that involved exposing the substrate in a steam environment at 1000°C for about 7 hours (Fig. 2(b)). A square opening of 1800 μm x 1800 μm was made in the SiO_2 layer by a dissolving agent in a typical photolithographical process (Fig. 1(c)). A thin membrane with a thickness of 100 μm was made in the silicon substrate using wet etching technique. The cross-section of the finished cavity and the membrane is shown in Fig 1d.

While the algorithms of A- and S-elements described in the foregoing section are still being developed, ANSYS 5.4 code with "birth" and "death" element features were used for the stress analysis. The "birth elements" have a similar effect as the "A-elements", whereas the "Death elements" are similar to the "S-elements". A major difference between the two approaches, however, is that both "A" and "S-elements" allow gradual change in element stiffness with corresponding adjustment of the $[B]$ matrices. Such features would allow more smooth transitions in stress/strain variations in adding and subtracting materials during the process.

The finite element mesh for the case study involved a total of 25,678 8-node solid elements and 29,696 nodes. The "birth" elements were used for oxidation whereas the "death" elements were used in the subsequent etching process. As a first attempt, all material properties are assumed to be temperature-independent. Input material properties are tabulated as follows:

	Silicon	**SiO_2**
Young's modulus (MPa)	195,000	73,000
Density (Kg/mm^2)	2.33×10^{-6}	2.27×10^{-6}
Poisson's ratio	0.3	0.28
Linear thermal expansion coefficient (1/°C)	3.5×10^{-6}	0.5×10^{-6}

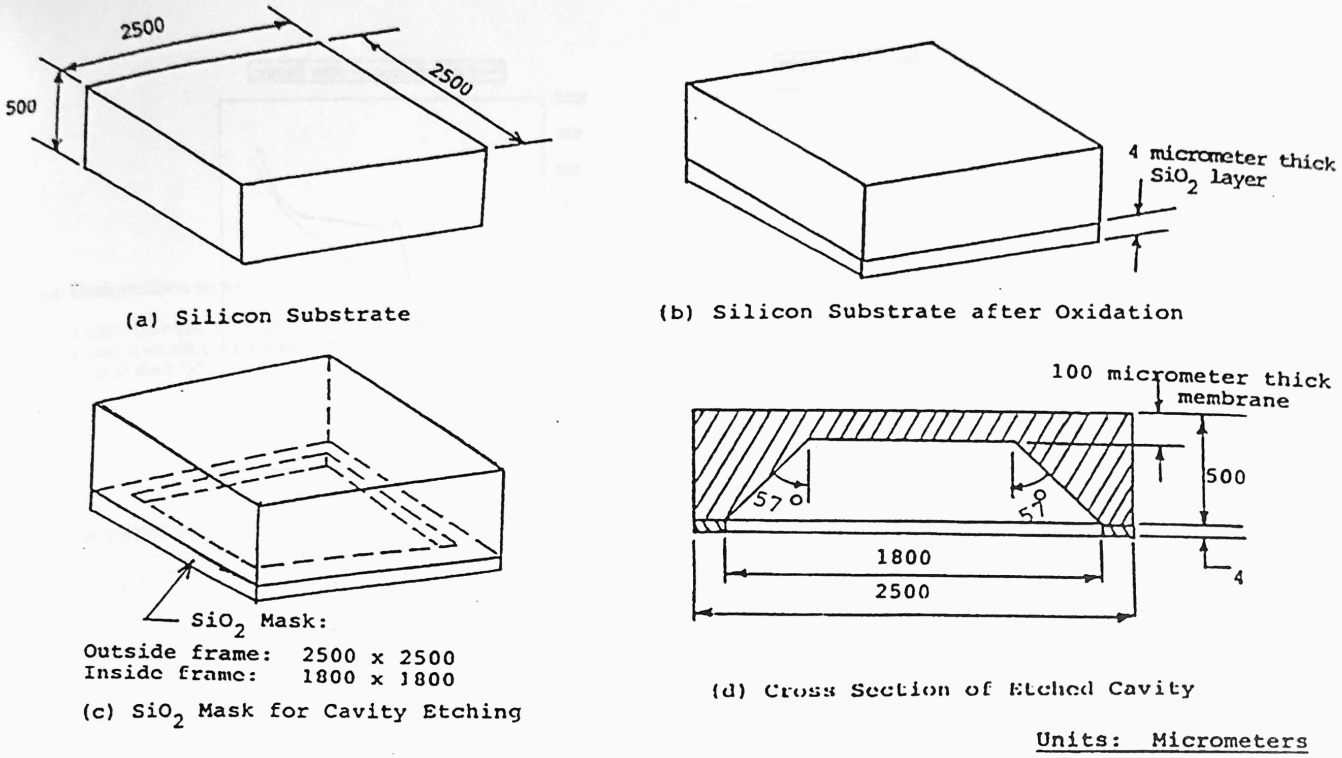

Fig. 1. Geometric Description of Case Study

Finite Element Results on Case Study

Results from the finite element analysis have shown substantial residual stresses and strains induced in the membrane structure by the fabrication process. Fig. 2 shows the effective stress distributions near both the top and bottom surfaces of the membrane before and after the etching of the cavity. The same stress distributions across the diagonal of the square membrane are shown in Fog. 3. Fig. 4 shows the contours of effective stress in half of the cross section of the membrane after etching. Normal stress distributions near the top and bottom surfaces of the membrane along the width before and after etching are shown in Fig. 5. Variation of residual effective strain in the membrane cross section is shown in contour plot in Fig. 6. The maximum effective strain of 1.6% was found near the center of the membrane.

Discussion on Results

The present case study has demonstrated the significance of residual stress and strain induced in MEMS device by simple processes. More complicated processes involving multi-layers structure would further complicate the situation with the needs to account for interfacial fracture strength. The residual stresses and strains at interfacial could be more severe due to mismatch of material properties.

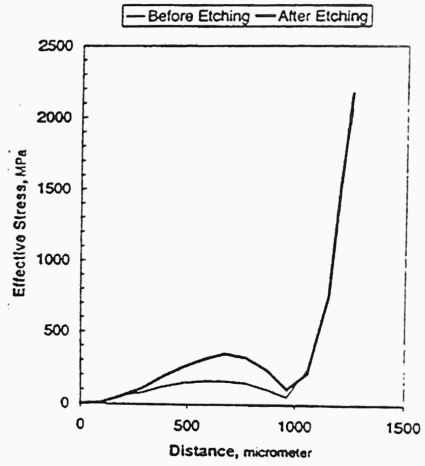

(a) Near top surface

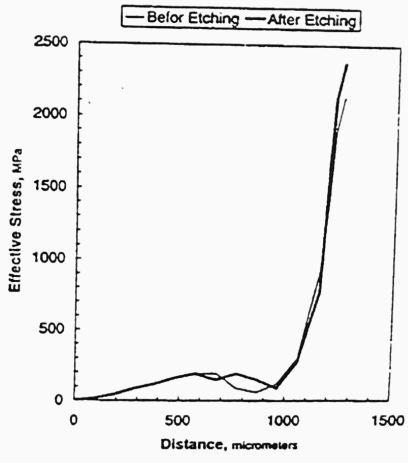

(b) Near bottom surface

Fig. 2. Distribution of Effective Stresses in Membrane along the Width

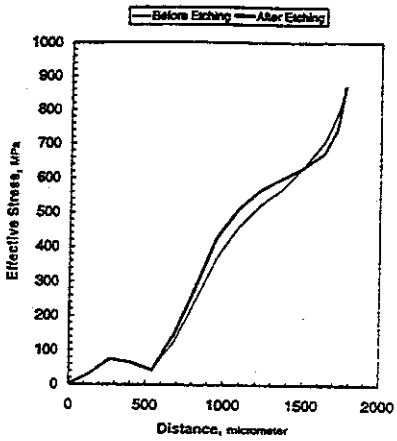

(a) Near top surface

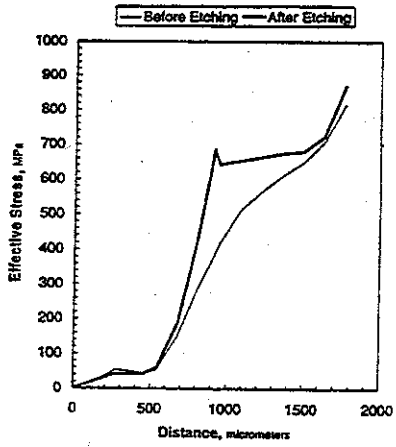

(b) Near bottom surface

Fig. 3 Distribution of Effective Stresses in Membrane along the Diagonal

Contour Designations (in MPa):

B = 100, C = 200, D = 300, E = 400, F = 500, J = 900, K = 1000, L = 1100
M = 1200, N = 1300, P = 1500, Q = 1600, R = 1700, S = 1800, U = 2000

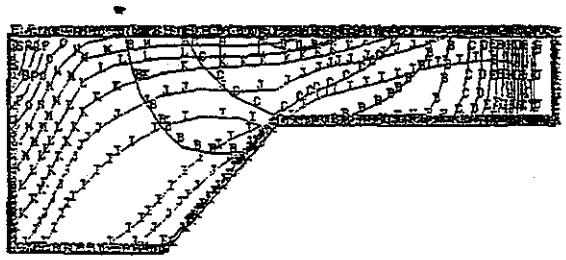

Fig. 4 Residual Effective Stress Distribution in Half Membrane Cross Section

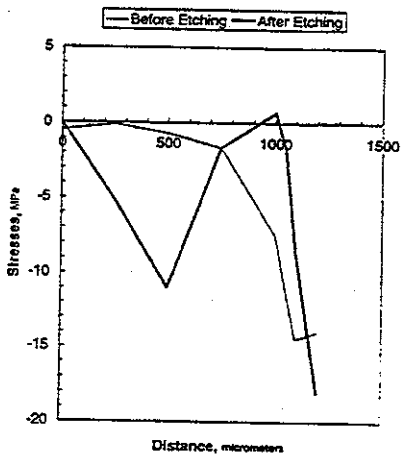

(a) Near top surface

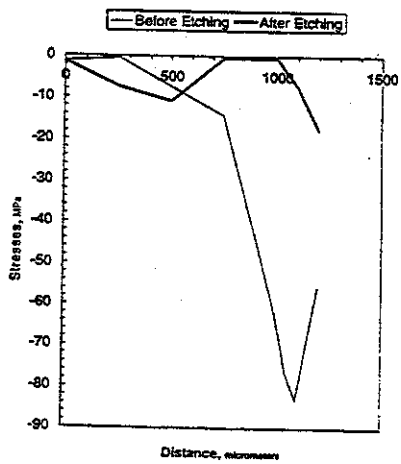

(b) Near bottom surface

Fig. 5 Distribution of Normal Stresses in Membrane along the Width

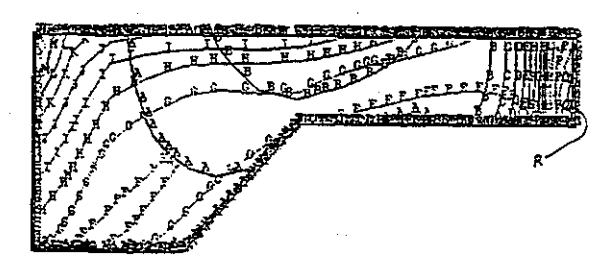

Fig. 6. Residual Effective Strain Distribution in Half Membrane Cross Section after Etching

to the stresses and strains induced in the structure were the respective thermal components. The temperature-independent material properties used in computations. For example, the major contribution thermal stresses are related to $\alpha E \Delta T$ and thermal strains are related to $\alpha \Delta T$, in which α, E, and ΔT are corresponding linear thermal expansion coefficients, Young's' moduli of the bi-layer materials and the temperature difference between the oxidation temperature and room temperature. In the current case study, the significant drop of Young' modulus of both materials at the "oxidation temperature", 1000°C could significantly reduce the thermal stresses. Likewise, the drop of linear thermal expansion coefficients of the materials from high temperature to the room temperature would also have significant effect on the results. These factors need to be included in a more precise analysis in a real case design.

The computational effort in this case study was quite substantial. The use of finite element analysis, though is necessary, requires enormous engineer's time in developing the discretized mesh, input data and evaluation of the output results. This action is thus recommended for design verification purpose only. Much effort in design methodology without having to use the finite element analysis is urgently needed.

REFERENCES

1. Friedrich, C.R., Fang, J., Warrinton, R.O. "Micromechatronics and the Miniaturization of Structures, Devices, and Systems," IEEE Transactions on Components, Packaging, and Manufacturing Technology, Part C, Vol. 20, No. 1, January, 1997, pp. 31-38.
2. Weiss, S.A. "Think Small: Laser compete in micromachining," Photonics Spectra, October, 1995, pp. 108-114.
3. O'connor "MEMS: Microelectromechanical Systems," Mechanical Engineering, February, 1992, pp. 40-47.
4. Pourahmadi, F. and Twerdok, J.W. "Modeling Micromachined Sensors with Finite Elements," Machine Design, July, 1990.
5. Senturia, S.D., Harris, R.M., Johnson, B.P., Kim, S., Nabors, K., Shulman, M.A. and White, J.K., "A CAD System for MEMS (MEMCAD),", IEEE/ASME Journal of MEMS, VOl. 1, No. 1, March, 1992, pp. 3-13.
6. "MEMS Assembly and Performance," Mechanical Engineering, August, 1997, pp. 16.
7. von Alvensleben, F., Gonschior, M., Kappel, H. and Heekenjann "Laser Micromachining," Optics & Photonics News, August, 1995, pp. 23-27.
8. Petersen, K.E., Barth, P.W., Poydock, J., Brown, J., Mallon, J. and Bryzek, J. "Silicon Fusion Bonding for Pressure Sensors," Proceedings of IEEE Solid-State Sensor and Actuator Workshop, Hilton Head, NC, 1988, p. 144.
9. Hsu, T.R. and Trasi, S.R. "On the Analysis of Residual Stress Induced in Sheet Metal by Thermal Shock Treatment," Journal of Applied Mechanics, ASME Transactions, March, 1976, pp. 117-123.
10. Bryzek, J., Petersen, K. and McCulley, W. "Micromachines on the March," IEEE Spectrum, May, 1994, pp. 20-31.
11. Madou, M. "Fundamentals of Microfabrication," CRC Pross, Boc Raton, 1997, p. 159.
12. Hsu, T.R. "The Finite Element Method in Thermomechanics," Allen & Unwin, London, 1986, Ch. 2,3,4,7 and 9.
13. Kim, Y.J. and Hsu, T.R. "A Numerical Analysis on Stable Crack Growth Under Increasing Load," International Journal of Fracture," VOl. 20. 1982, pp. 17-32.
14. Sun, N.S. and Hsu, T.R. "Thermomechanical Coupling Effects on Fractured Solids,", International Journal of Fracture, Vol. 78, 1996, pp. 67=86.